

Reactions of coordinated polyolefins *. Kinetic studies of a fluxional [2,2]-sigmahaptotropic rearrangement by the spin saturation transfer technique and line shape analysis

Zeev Goldschmidt * and Hugo E. Gottlieb

Department of Chemistry, Bar-Ilan University, Ramat-Gan 52100 (Israel)

(Received June 15th, 1988)

Abstract

The reaction of (3,7,7-trimethylcycloheptatriene)tricarbonyliron with tetracyanoethylene gave an equilibrium mixture of the 2 + 2 and 3 + 2 isomeric adducts in a 2/3 ratio. The rate constants for the interconversion process in CDCl_3 were evaluated by the spin saturation transfer technique, and in CD_3OD by line shape analysis. The activation parameters were ΔH^\ddagger 15 kcal/mol, ΔS^\ddagger -10 e.u. (CDCl_3), and ΔH^\ddagger 20 kcal/mol, ΔS^\ddagger +12 e.u. (CD_3OD), respectively. The kinetic data is consistent with a mechanism in which isomerization proceeds via a single step pericyclic [2,2]-sigmahaptotropic rearrangement.

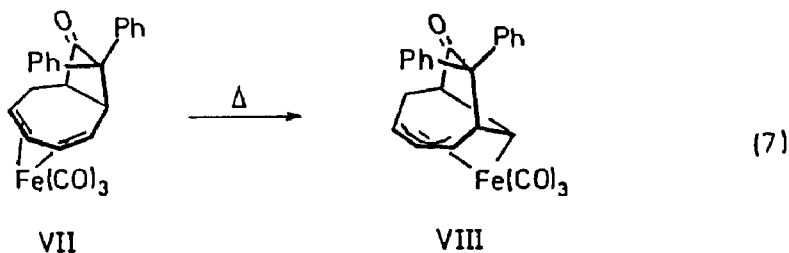
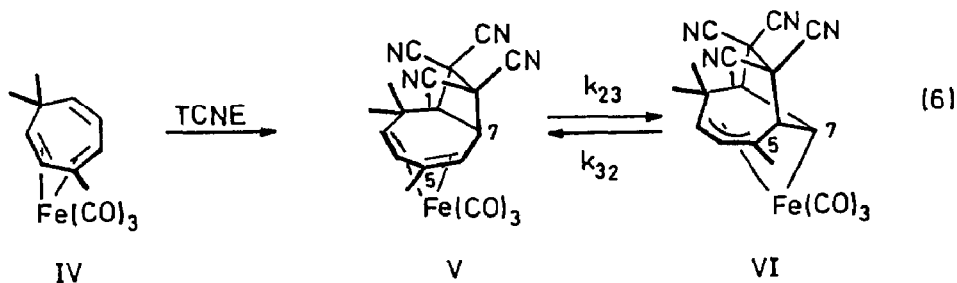
Introduction

Acyclic 1,1-disubstituted butadienes and hexatrienes react efficiently with tetracyanoethylene (TCNE) to give a mixture of the 2 + 2 and 4 + 2 (Diels–Alder) adducts (eq. 1, 2) [2,3]. The ratio between the products is solvent dependent, favoring the vinylcyclobutane 2 + 2 adduct in more polar solvents. Some of the butadiene 2 + 2 adducts are kinetically labile, isomerizing via a formal 1,3-sigmatropic migration to the corresponding cyclohexene 4 + 2 adducts [2a].

η^4 -Coordinated acyclic trienes react with TCNE solely in the 2 + 2 manner, via the noncoordinated double bond (eq. 3) [4].

In the cyclic series, cycloheptatriene (cht) enters into the Diels–Alder reaction with TCNE by way of its norcaradiene valence isomer (eq. 4) [5], and no other products are formed. However, the corresponding $(\eta^4\text{-cht})\text{Fe}(\text{CO})_3$ complex (I), unlike its acyclic hexatriene counterpart, reacts with TCNE to give initially the 3 + 2

* For previous paper in this series see ref. 1.



adduct (VI), the interconversion occurring via a [2,2]- $\sigma\eta$ rearrangement [1] (eq. 6). The results of structural and kinetic studies of this reaction are the subject of the present paper.

Results

The reaction of IV and TCNE was carried out in CHCl_3 as described before [8]. The ^1H NMR spectrum of the recrystallized product in CDCl_3 shows the presence of two isomers in a ca. 2/3 ratio. This ratio remained constant at room temperature or when the solution was kept at 50°C for several hours. A similar constant ratio between the isomers was observed in methanolic solutions. Repeated recrystallizations did not change the observed ratio, clearly indicating the existence of an equilibrium between the two isomers. An unequivocal confirmation of the presence of this equilibrium resulted from $^1\text{H}\{^1\text{H}\}$ double irradiation experiments. For example, irradiation at the frequency of H(7)(V) caused not only the expected decoupling of the neighboring H(1)(V) and H(6)(V) but also a decrease in the intensity of the signal from H(7)(VI) (Fig. 1), indicating spin saturation transfer (SST). We consequently took advantage of this phenomenon to calculate the kinetic rate constants, using the method developed by Hoffman and Forsen [9] (*vide infra*).

In methanol as a solvent, the interconversions involved into equilibrium are faster than in chloroform, causing a significant broadening of the proton lines even at room temperature. Hence the more convenient line shape analysis technique [10] was used at several temperatures (*vide infra*).

Details of the ^1H NMR spectroscopic data for isomers V and VI are given Table 1. Spectral data for the analogous 2 + 2 (VII) and 3 + 2 (VIII) adducts of I with diphenyl ketene [1] (eq. 7), and for the TCNE 6 + 2 adduct III [7] are also listed in

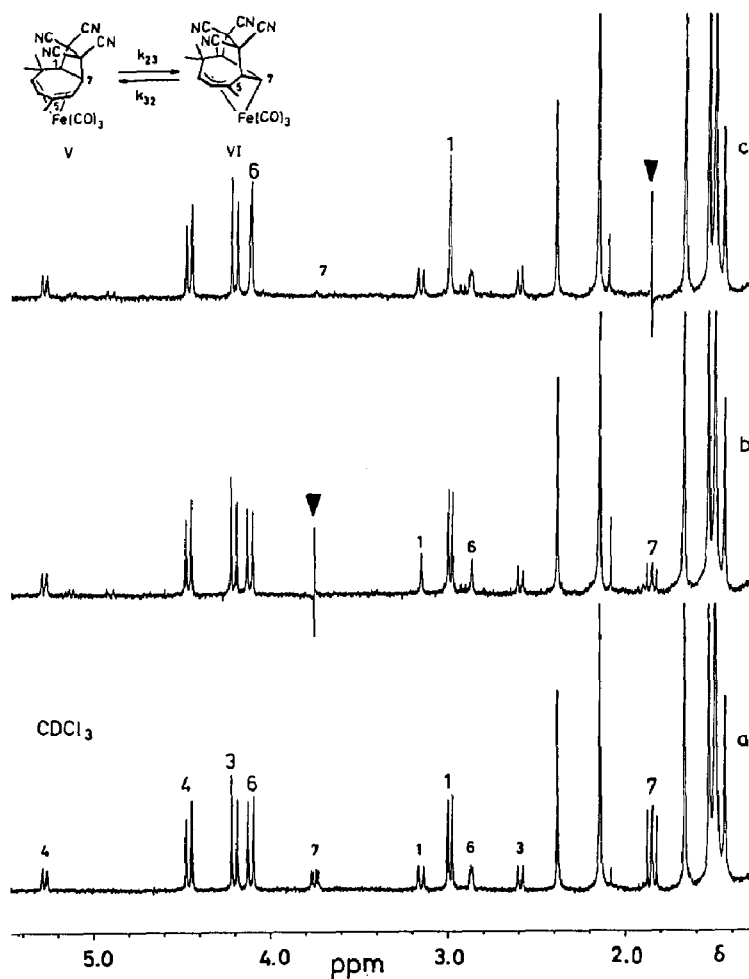


Fig. 1. ^1H NMR spectrum of $\text{V} \rightleftharpoons \text{VI}$ in CDCl_3 . (a) Not irradiated. Smaller numbers indicate signals of V, larger numbers of VI. For assignment of the methyl signals see Table 1. (b) Irradiation of $\text{H}(7)(\text{V})$. (c) Irradiation of $\text{H}(7)(\text{VI})$.

Table 1 for comparison. Extensive decoupling experiments revealed the carbon connectivity shown in Table 1, whereas the excellent correlation of the coupling constants (J) of the two isomers with those of the corresponding diphenyl ketene adducts VII and VIII established unequivocally the cyclobutane and σ, π -allylic structures of V and VI, respectively.

Kinetics

The exchange rates (k_{AB}) in CDCl_3 solutions were measured by the Fourier transform version of the Hoffman–Forsen SST method [9]. Thus, if A and B are nuclei in the two species which are interconverted by the exchange process, then

$$1/\tau = k_{\text{AB}} + (1/T_1) \quad (8)$$

$$r = (1/T_1) / [k_{\text{AB}} + (1/T_1)] \quad (9)$$

Table 1

¹H NMR spectroscopic data for cycloheptatrieneticarbonyliron adducts ^a

Compound	solvent	H(1)	H(2s)	H(2a)	H(3)	H(4)	H(5)	H(6)	H(7)
V	CD ₃ OD	3.59	1.33* ^b	1.47*	2.85	5.52	2.38*	3.20	4.13
	CDCl ₃	3.16	1.24*	1.44*	2.60	5.28	2.38*	2.87	3.77
^c J_{13} 1.2, J_{16} 0.8, J_{17} 9.3, J_{34} 8.2, J_{46} 1.3, J_{67} 3.5									
VI	CD ₃ OD	3.44	1.61*	1.65*	4.46	4.84	2.24*	4.65	2.00
	CDCl ₃	3.00	1.53*	1.66*	4.21	4.47	2.15*	4.13	1.84
^c J_{13} 0.7, J_{16} 1.1, J_{17} 7.3, J_{34} 9.5, J_{46} 1.1, J_{67} 7.5									
VII	(CD ₃) ₂ CO	3.39	2.07	2.43	3.15	5.31	4.82	2.94	4.01
aromatic: 7.20–7.55 J_{12a} 8.3, J_{12a} 1.5, J_{16} 0.9, J_{17} 10.4, J_{22} 17.8, J_{2a3} 2.8, J_{2a3} 5.1, J_{2a4} 1.3, J_{2a7} 0.3, J_{34} 8.1, J_{35} 1.5, J_{45} 5.3, J_{46} 0.9, J_{56} 7.8, J_{67} 4.3									
VIII	C ₆ D ₆	2.52	2.84	2.86	4.60	4.20	4.01	4.07	1.99
		aromatic: 6.98 (o), 7.19–7.31 (m,p) J_{12a} 9.0, J_{12a} 3.0, J_{13} ~ 0.5, J_{16} 1.0, J_{17} 9.0, J_{22} 16.0, $J_{2a3} = J_{2a3}$ 3.0, J_{2a4} 0.5, J_{34} 9.3, J_{45} 7.8, J_{56} 6.5, J_{57} 2.1, J_{67} 7.0							
III	(CD ₃) ₂ CO	3.97	1.60	2.08	3.97	3.81	5.91	5.91	3.81
	CDCl ₃	3.59	1.52	2.06	3.59	3.52	5.72	5.72	3.52
^d $J_{12a} = J_{2a3}$ 1.3, $J_{12a} = J_{2a3}$ 4.1, $J_{17} = J_{34}$ 9.5, J_{22} 14.0, $J_{2a4} = J_{2a7}$ 0.8, ^e J_{13} 2.0, $J_{2a5} = J_{2a6}$ 0.3, $J_{45} = J_{67}$ 9.0, $J_{46} = J_{57}$ 2.0, J_{47} 0.5, J_{56} 5.0									

^a δ (ppm) from TMS; J (Hz). ^b numbers marked with * refer to methyl signals; s = *syn*, a = *anti* (to the metal); numbering as in text. ^c In CD₃OD. ^d In (CD₃)₂CO. ^e These coupling constants were obtained by fitting to calculated spectra using Bruker's PANIC simulation program.

where T_1 is the spin-lattice relaxation time of nucleus A, τ is the spin lifetime of A (including the relaxation and chemical exchange processes), k_{AB} is the kinetic rate constant for the A \rightarrow B exchange process, and r is the ratio between the intensities of the A signal, with and without irradiation of B, respectively. Equations 8 and 9 can be combined to give:

$$k_{AB} = (1 - r) / \tau \quad (10)$$

Equation 10 permits the calculation of k_{AB} , since the value of r is readily measured from the integrals of the double-irradiated spectrum, and τ is obtained by the usual inversion-recovery experiment (180°- t -90°-acq.) [11] (Fig. 2a), in which the signal of B is continuously irradiated to cancel the contribution of the back-exchanging nuclei (B \rightarrow A).

The kinetic data for the [2,2]- $\sigma\eta$ rearrangement in CDCl₃ are listed in Table 2. Measurements are based on the exchange process between the two H(7) nuclei. In these inversion-recovery experiments the signal of H(7)(VI) was integrated while H(7)(V) was continuously irradiated.

The variable temperature line shape analysis (LSA) [10] was employed for the kinetic studies in CD₃OD. The peaks selected for this study were the well-isolated 5-methyl signals at δ 2.15 (VI) and 2.38 (V) (Fig. 1). At 22°C these appear as two quite sharp singlets and broaden as the temperature is raised to 50°C without

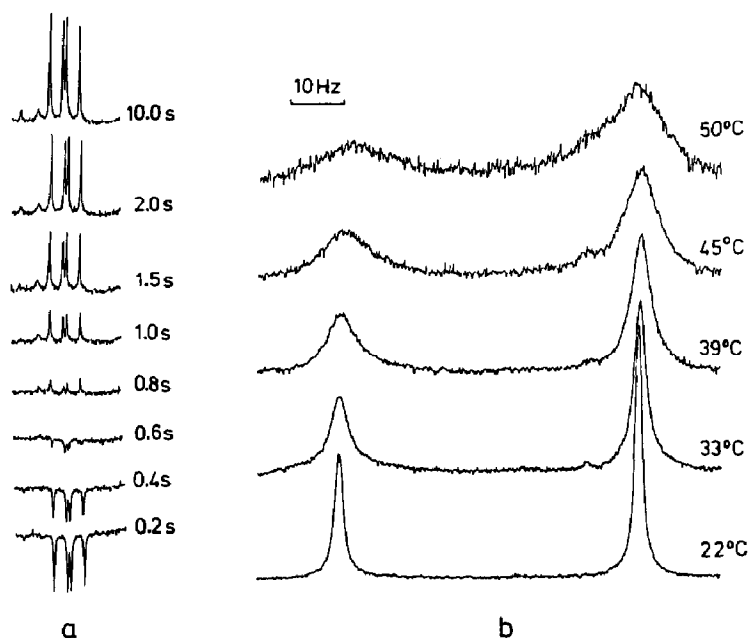


Fig. 2. Reaction kinetics by SST (a) and LSA (b) techniques. (a) Inversion-recovery (180° - t - 90° -acq.) experiment; H(7)(VI) signal (CDCl_3 , 40°C , t in seconds). (b) Variable temperature line shape of the 5-methyl signals (CD_3OD).

Table 2

Kinetic data for the [2,2]-sigmahaptotropic rearrangement by spin saturation transfer (in CDCl_3)

T (K)	τ_7 (s) ^a	r ^a	k_{32} (s^{-1})	ΔG^\ddagger (kcal/mol)	K_{eq} ^a
297	1.42	0.73	0.19 ± 0.03	18.37 ± 0.10	3.7
302	1.21	0.63	0.30 ± 0.03	18.38 ± 0.08	3.1
307	1.06	0.50	0.48 ± 0.04	18.43 ± 0.07	3.0
316	0.66	0.36	0.97 ± 0.06	18.57 ± 0.06	3.1

$\Delta H^\ddagger = 15.1 \pm 0.6$ kcal/mol, $\Delta S^\ddagger = -11 \pm 3$ e.u.

^a The estimated errors are ± 0.01 s for τ , ± 0.04 for r , and ± 0.7 for K_{eq} .

Table 3

Kinetic data for the [2,2]-sigmahaptotropic rearrangement by line shape analysis (in CD_3OD).

T (K)	hw ^a (Hz)	k_{23} (s^{-1})	ΔG^\ddagger (kcal/mol)	hw ^b (Hz)	k_{32} (s^{-1})	ΔG^\ddagger (kcal/mol)
295	0.6 ± 0.2	1.9 ± 0.6	16.89 ± 0.20	0.4 ± 0.2	1.3 ± 0.6	17.13 ± 0.27
300	1.0 ± 0.2	3.1 ± 0.6	16.86 ± 0.14	0.8 ± 0.2	2.5 ± 0.6	16.99 ± 0.16
304	2.0 ± 0.2	6.3 ± 0.6	16.71 ± 0.09	1.3 ± 0.2	4.1 ± 0.6	16.97 ± 0.12
307	2.9 ± 0.3	9.1 ± 0.9	16.61 ± 0.09	1.7 ± 0.3	5.3 ± 0.9	16.94 ± 0.13
312	5.2 ± 0.4	16.3 ± 1.3	16.57 ± 0.08	3.3 ± 0.4	10.4 ± 1.3	16.85 ± 0.10
318	8.2 ± 0.5	25.8 ± 1.6	16.60 ± 0.06	5.8 ± 0.5	18.2 ± 1.6	16.81 ± 0.08
324	13.5 ± 0.7	42.4 ± 2.2	16.58 ± 0.05	10.2 ± 0.7	32.0 ± 2.2	16.76 ± 0.08

ΔH^\ddagger 20.3 ± 0.6 kcal/mol

ΔS^\ddagger 12 ± 3 e.u.

ΔH^\ddagger 20.7 ± 0.6 kcal/mol

ΔS^\ddagger 12 ± 3 e.u.

^a Corrected line width, 5-Me(V). ^b Corrected line width, 5-Me(VI).

reaching coalescence (Fig. 2b). Thus, over this temperature range, the rate constants for the rearrangement (k_{AB}) are simply proportional to the corrected linewidths (eq. 11) [10]. The kinetic data are shown in Table 3.

$$k = \pi \nu_{1/2} \quad (11)$$

Discussion

Although there are a few examples in the literature of rearrangement of 2 + 2 vinylcyclobutane adducts of TCNE with 1,3-dienes to the isomeric 4 + 2 (Diels–Alder) adducts in uncoordinated compounds [2a], the present example is to our knowledge the first in which a 2 + 2 adduct is found to be in equilibrium with its isomeric counterpart (in this case the 3 + 2 adduct). We recently described a closely related [2,2]- $\sigma\eta$ reaction, in which 2 + 2 adducts of (cht)Fe(CO)₃ (I) and aryl ketenes rearrange to the corresponding 3 + 2 isomers (eq. 7) [1]. In the latter case we had both kinetic and steric evidence that the rearrangement is a thermally allowed pericyclic reaction, involving a concerted process in which a σ -bonded carbon and a metal fragment exchange bonding sites about a C–C σ bond [12].

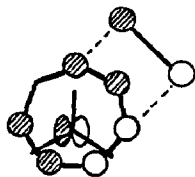
The present kinetic data are also consistent with a concerted mechanism. We note particularly the low activation energies in both chloroform (ΔH^\ddagger 15.1 kcal/mol) and methanol (ΔH^\ddagger 21 kcal/mol), and the moderate solvent effect, $k_{rel} = k(\text{methanol})/k(\text{chloroform}) = 9.5$ at room temperature, which are typical for pericyclic $\sigma\eta$ -rearrangements [1,7,12]. The positive value of ΔS^\ddagger +12 e.u. in methanol is somewhat surprising in light of previous results obtained for the related $\sigma\eta$ -reactions in methanol [1] and other solvents [7,12], for which the activation entropies are negative. This may indicate that in methanol, unlike in chloroform, the transition state to the rearrangement is less constrained than the reactants.

In order to confirm that both the forward and backward reactions occur in a single kinetic step and not by a stepwise cycloaddition-cycloreversion reaction, (carbomethoxy)maleic anhydride (CMA) was added to the equilibrium mixture. None of the expected adducts of (cht)Fe(CO)₃ with CMA [13] was detected. Hence, a two step rearrangement in either direction can be excluded.

It is interesting to note that while the 3 + 2 adduct of the unsubstituted (cht)Fe(CO)₃ with TCNE (II) undergoes a thermal rearrangement to give exclusively the 6 + 2 isomer III, the trimethyl-substituted 6 + 2 counterpart does not show a comparable thermal stability. In contrast, the 2 + 2 trimethyl adduct V is less stable than its 3 + 2 isomer VI by ca. 0.77 kcal/mol (at 24°C). Since the 2 + 2 and 6 + 2 isomers are both η^4 -butadiene complexes, expected to be of similar stabilities, the reason for the preference of the more strained cyclobutane system in the trimethyl series probably results from steric effects caused by one or both *gem* dimethyl groups at position 2.

Since the cycloaddition reaction is too fast to be followed by NMR spectroscopy at room temperature, it was not possible to determine experimentally which of the adducts is the primary product of the reaction. However, consideration of previous kinetic studies of cycloadditions in related cycloheptatriene derivatives suggests that these reactions are subject to frontier orbital control [6,12,13]. As such, the controlling interaction appears to involve the subjacent molecular orbital [12,13] of

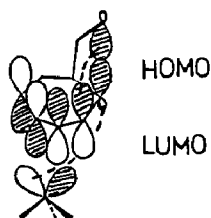
cycloheptatriene complex IV and the LUMO of TCNE, as depicted in IX. This implies the initial formation of the 3 + 2 adduct VI, which subsequently undergoes equilibration with its 2 + 2 isomer V via the [2,2]- $\sigma\eta$ rearrangement. However, the existence of several examples of two-step 2 + 2 (polar) cycloadditions of electron-rich ethylenes with TCNE [2,3,14] suggests that this pathway can not be entirely excluded.



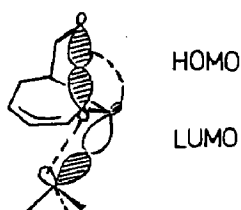
IX

We conclude by outlining the general mechanism of the pericyclic [2,2]-sigmatropic rearrangement, a reaction in which a σ -bond (e.g. C(7)–C(8) of V) and a carbon–metal bond (C(6)–Fe) interchange about a two carbon chain (C(6)–C(7)) [1]. In pentacoordinated complexes, this process involves a concerted suprafacial 1,2-sigmatropic shift and a metal (haptotropic) migration, along a symmetrical Berry pseudorotation pathway [15], within the metal coordination sphere. This is shown in Scheme 1b for the interconversion of the square pyramidal (*sp*) butadiene complex V and the σ,π -allylic trigonal bipyramid (tbp) VI. The molecular orbital correspondance picture, illustrated in Scheme 1a, shows the three bonds which participate in the [2,2]- $\sigma\eta$ rearrangement. These are the migrating σ -bond and the two organometal (mo) bonds obtained by interaction of the HOMO-LUMO pair of the $\text{Fe}(\text{CO})_3$ fragment (e orbitals) with the corresponding frontier orbitals of either a butadiene (π_2 , π_3^*) [16] or a σ,π -allylic system (p_c , π_n) [1,17]. Thus, the $\sigma_{22}(\text{C}(7)\text{--}\text{C}(8))$, $\pi(\pi_2 + e_{xy})$ and $\pi(e_{yz} + \pi_3^*)$ molecular orbitals of V correlate with the $\sigma_{32}(\text{C}(6)\text{--}\text{C}(8))$, $\sigma(p_c + e_{xy})$ and $\pi(e_{yz} + \pi_n)$ molecular orbitals of VI, respectively, as shown in Scheme 1a,c (a side view, c bottom view, R = migrating C(8) group). We note from Scheme 1b, that the pseudorotation plane (of the paper) contains three ligands, CO(1) as the pivot, CO(2), and π_{56} of the square pyramidal V. This, of course, is the same plane containing the pivot CO(1), CO(2), and C(7) ligands of the trigonal bipyramidal VI. A more comprehensive analysis of the [2,2]- $\sigma\eta$ rearrangement has recently been published elsewhere for the analogous ketene adducts [1].

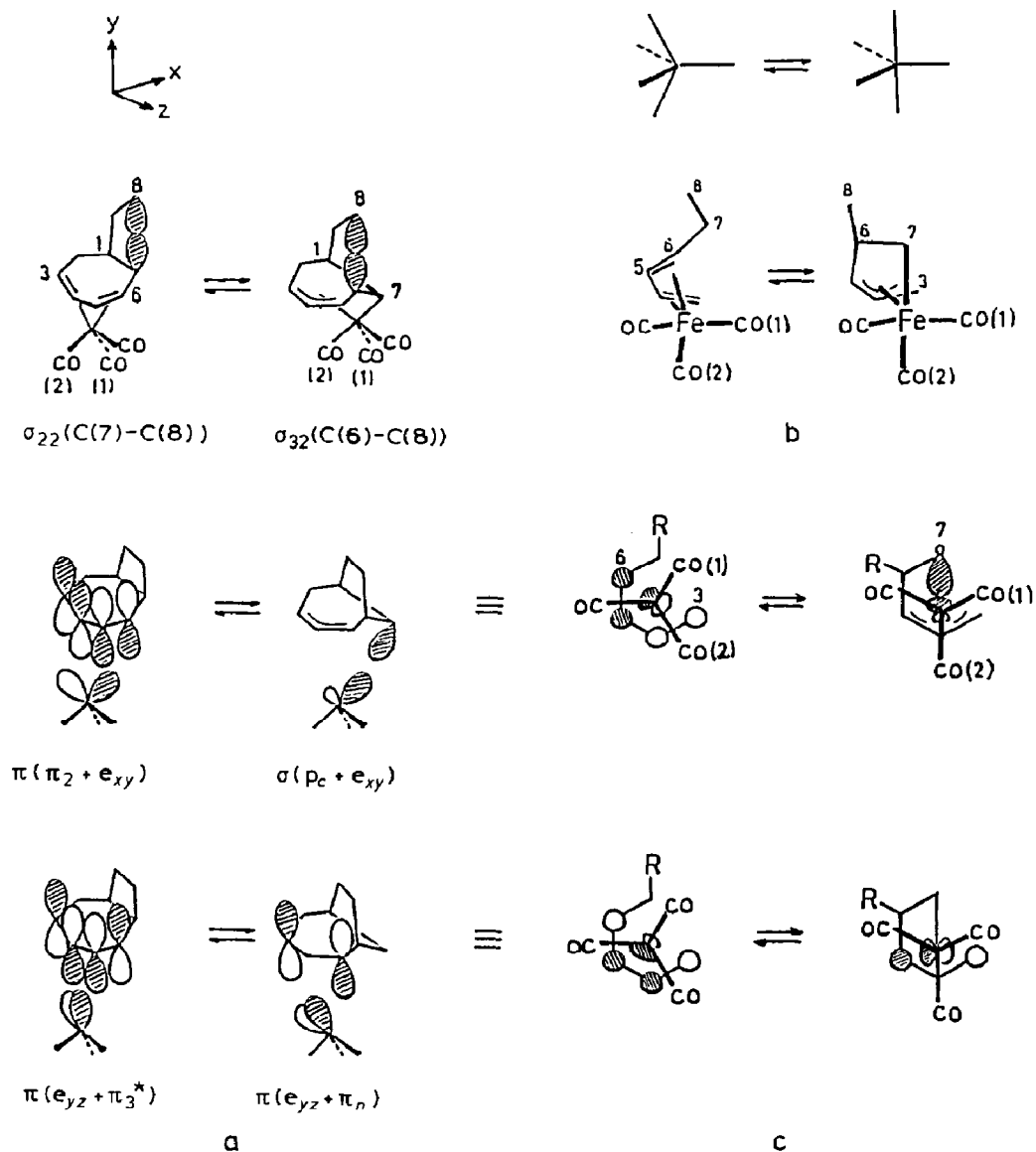
Alternatively, this rearrangement can also be represented as an intramolecular interaction of the $\sigma(\text{C}\text{--}\text{C})$ HOMO and the appropriate organometallic LUMO. This is shown in X for the V \rightarrow VI reaction [1] and in XI for the reverse VI \rightarrow V direction. Notice that the latter describes a formal interchange between two σ bonds about a C–C bond, and thus resembles the pericyclic 4-electron dyotropic reactions [18].



X

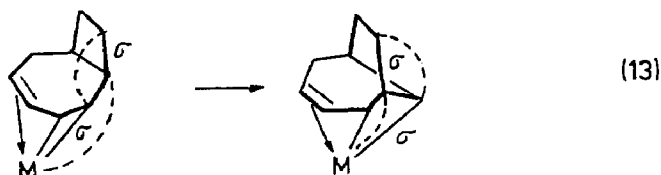
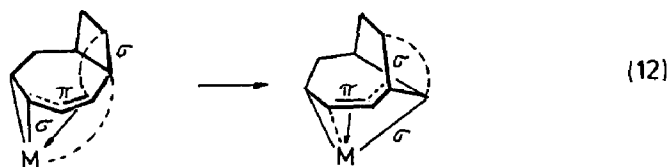


XI



Scheme 1. The [2,2]- $\sigma\eta$ rearrangement along a pseudorotation reaction pathway. (a) Orbital correlation diagram, side view. (b) Pseudorotation view in the plane of the paper. (c) Orbital correlation diagram (organometal orbitals only), bottom view, R = migrating group (C(8)).

Finally, it is also possible to analyze the [2,2]- $\sigma\eta$ rearrangement in terms of the Woodward–Hoffmann topological rules, using a valence bond representation of the organometallic bonding [1,19]. If we follow the molecular orbital analysis described in Scheme 1, then the reaction involves a 6-electron cyclic array of the type $\sigma 2a + (\sigma 2s + \pi 2a)_{\text{mo}}$, as shown in eq. 12. Alternatively, a 4-electron dyotropic process may be invoked, consistent with a thermally allowed $\sigma 2a + (\sigma 2s)_{\text{mo}}$ reaction (eq. 13).



Experimental

The complex (3,7,7-Trimethyl-cht)Fe(CO)₃ (IV) was prepared and treated with TCNE as described previously [8]. All the kinetic experiments were performed in NMR tubes. Dilute solutions (10–20 mM) of the crystalline adduct in CDCl₃ and CD₃OD were purged with nitrogen and were sufficiently stable throughout the period of the experiments.

Variable temperature NMR spectra were recorded on a Bruker AM300 spectrometer equipped with an ASPECT 3000 data system. The sample temperatures were measured with an Omega 870 digital thermometer, before and after each experiment; values are correct within $\pm 0.5^\circ\text{C}$.

In the SST experiments, the spin lifetimes were obtained from at least 6 time points, in addition to two "infinity" times ($t = 10$ s).

The linewidths for the LSA experiments were corrected both for the instrument resolution (from the TMS peak) and the long-range coupling of the 5-Me signals (from the spectrum in CDCl₃).

References

- 1 Z. Goldschmidt and H.E. Gottlieb, *J. Organomet. Chem.*, 329 (1987) 391.
- 2 (a) F. Kataoka, N. Shimizu and S. Nishida, *J. Am. Chem. Soc.*, 102 (1980) 711; (b) A.D. Josey, *Angew. Chem. Int. Ed. Eng.*, 20 (1981) 686.
- 3 For a recent review see: A.J. Fatiadi, *Synthesis*, (1987) 749.
- 4 Z. Goldschmidt and Y. Bakal, *J. Organomet. Chem.*, 269 (1984) 191.
- 5 N.W. Jordan and I.W. Elliot, *J. Org. Chem.*, 27 (1962) 1445; G.H. Wahl, *J. Org. Chem.*, 33 (1968) 2158.
- 6 M. Green, S. Heathcock and D.C. Wood, *J. Chem. Soc. Dalton Trans.*, (1973) 1563.
- 7 Z. Goldschmidt, H.E. Gottlieb, E. Genizi, D. Cohen and I. Goldberg, *J. Organomet. Chem.*, 301 (1986) 337.
- 8 Z. Goldschmidt and S. Antebi, *J. Organomet. Chem.*, 259 (1983) 119.
- 9 R.A. Hoffman and S. Forsen, *Prog. Nucl. Magn. Reson. Spectros.*, 1 (1966) 15; J.W. Faller in J.J. Zuckerman and F.C. Nachod (Eds.), *Determination of Organic Structures by Physical Methods*, Academic Press, New York, 1973, Vol. 5; B.E. Mann, *Prog. Nucl. Magn. Reson. Spectrosc.*, 11 (1977) 95.

- 10 I.O. Sutherland, *Ann. Rep. NMR Spectros.*, 4 (1971) 71; G. Binsch in J.M. Jackman and F.A. Cotton (Eds.), *Dynamic Nuclear Magnetic Resonance Spectroscopy*, Academic Press, New York, 1968, Chap. 3, p. 45.
- 11 See e.g.: E.D. Becker, *High Resolution NMR*, Academic Press, New York, 1980, p. 232; H. Gunther, *NMR Spectroscopy*, John Wiley, Chichester, 1980, p. 225.
- 12 Z. Goldschmidt, H.E. Gottlieb and D. Cohen, *J. Organomet. Chem.*, 294 (1985) 219.
- 13 Z. Goldschmidt, S. Antebi, H.G. Gottlieb, D. Cohen, U. Shmueli and Z. Stein, *J. Organomet. Chem.*, 282 (1985) 369.
- 14 P.D. Bartlett, *Quart. Rev. (London)*, 24 (1970) 473; R. Huisgen, *Acc. Chem. Res.*, 10 (1977) 117.
- 15 A. Rossi and R. Hoffmann, *Inorg. Chem.*, 14 (1975) 365; R.S. Berry, *J. Chem. Phys.*, 32 (1960) 933.
- 16 T.A. Albright, R. Hoffmann, and P. Hofmann, *Chem. Ber.*, 111 (1978) 1591; M. Elian and R. Hoffmann, *Inorg. Chem.*, 14 (1975) 1058.
- 17 B.E.R. Schilling, R. Hoffmann and J.W. Faller, *J. Am. Chem. Soc.*, 101 (1979) 592; M.D. Curtis and O. Eisenstein, *Organometallics*, 3 (1984) 887.
- 18 M.T. Reetz, *Adv. Organomet. Chem.*, 16 (1977) 33; Z. Goldschmidt and S. Antebi, *Tetrahedron Lett.*, (1978) 271.
- 19 D.M.P. Mingos, *J. Chem. Soc. Dalton Trans.*, (1977) 31; M. Green, S.M. Heathcock, T.W. Turney and D.M.P. Mingos, *ibid.*, (1977) 204.